Engineering Conferences International
ECI Digital Archives

BioEnergy IV: Innovations in Biomass Conversion for Heat, Power, Fuels and Chemicals

Proceedings

Spring 6-10-2013

A CFD study of gas-solid separation in a downer pyrolysis reactor: An eulerian-eulerian approach

Xi Yu
Aston University

Yassir Makkawi
European Bioenergy Research Institute (EBRI), School of Engineering and Applied Science, Aston University

Follow this and additional works at: http://dc.engconfintl.org/bioenergy_iv

Part of the Chemical Engineering Commons

Recommended Citation
Xi Yu and Yassir Makkawi, "A CFD study of gas-solid separation in a downer pyrolysis reactor: An eulerian-eulerian approach" in "BioEnergy IV: Innovations in Biomass Conversion for Heat, Power, Fuels and Chemicals", Manuel Garcia-Perez,Washington State University, USA Dietrich Meier, Thünen Institute of Wood Research, Germany Raffaella Ocone, Heriot-Watt University, United Kingdom Paul de Wild, Biomass & Energy Efficiency, ECN, The Netherlands Eds, ECI Symposium Series, (2013). http://dc.engconfintl.org/bioenergy_iv/9

This Conference Proceeding is brought to you for free and open access by the Proceedings at ECI Digital Archives. It has been accepted for inclusion in BioEnergy IV: Innovations in Biomass Conversion for Heat, Power, Fuels and Chemicals by an authorized administrator of ECI Digital Archives. For more information, please contact franco@bepress.com.

A CFD STUDY OF GAS-SOLID SEPARATION IN A DOWNER PYROLYSIS REACTOR: AN EULERIAN-EULERIAN APPROACH

Speaker: Dr Xi Yu &Dr Yassir T. Makkawi
European Bioenergy Research Institute (EBRI), School of Engineering and Applied Science, Aston University, Birmingham B4 7ET, United Kingdom

Outlines

1. Biomass pyrolysis and downer pyrolysis reactor
2. Objectives and CFD model
3. Results and discussion
4. Summary and Acknowledgement

BioFuel and Biochar in one step

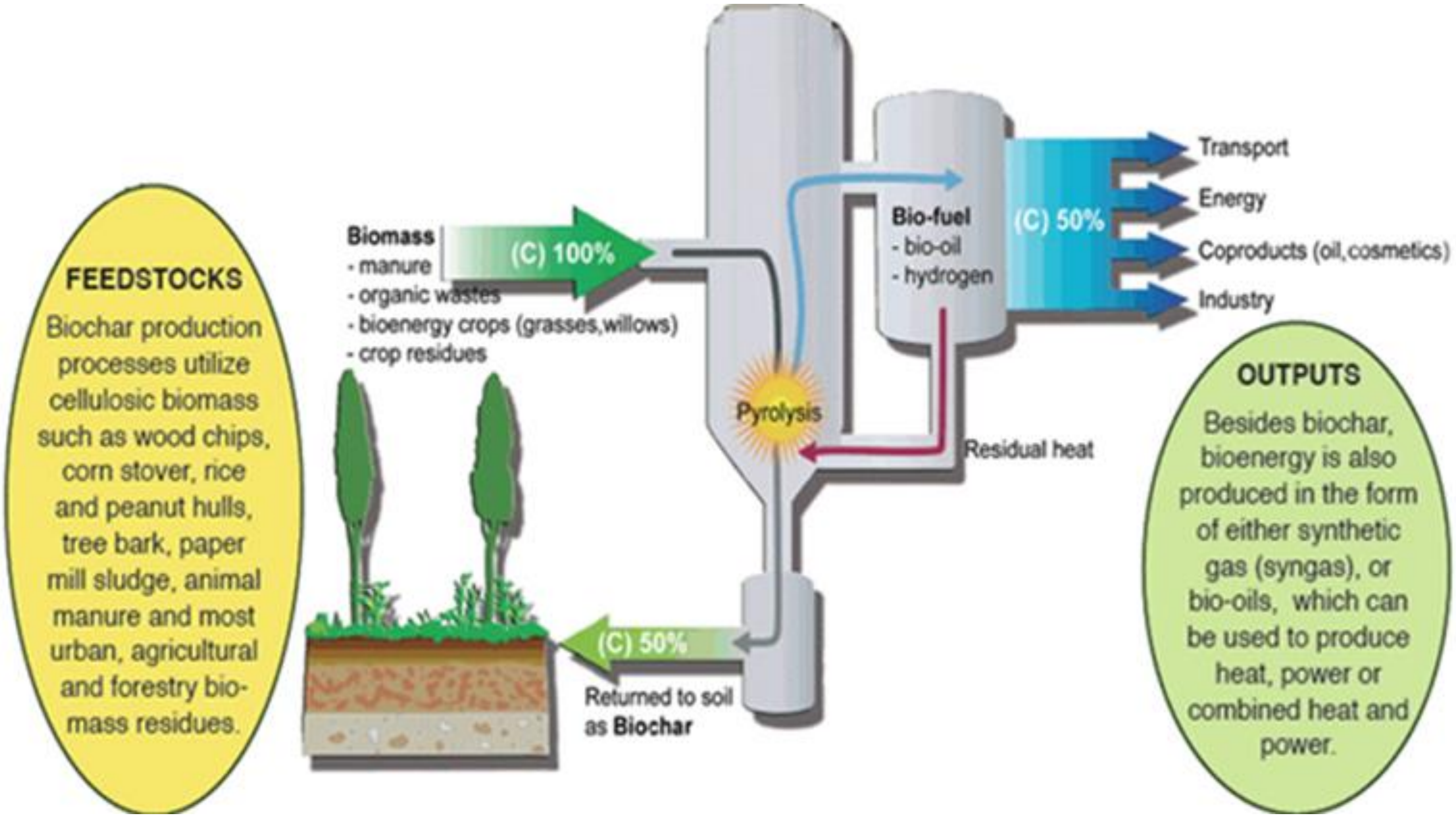

Pyrolysis is a thermochemical decomposition of organic material at elevated temperatures without the participation of oxygen.

Biomass Pyrolysis Products-*importance of residence time*

	Liquid	Char	Gas
Fast pyrolysis **Moderate temperature** **Short residence time**	**75%**	**12%**	**13%**
Carbonisation **Low temperature** **Long residence time**	**30%**	**35%**	**35%**
Gasification **High temperature** **Long residence time**	**5%**	**10%**	**85%**

Source: Review of Fast Pyrolysis of Biomass, Stefan Czernik, National Renewable Energy Laboratory

Novel gas separation method

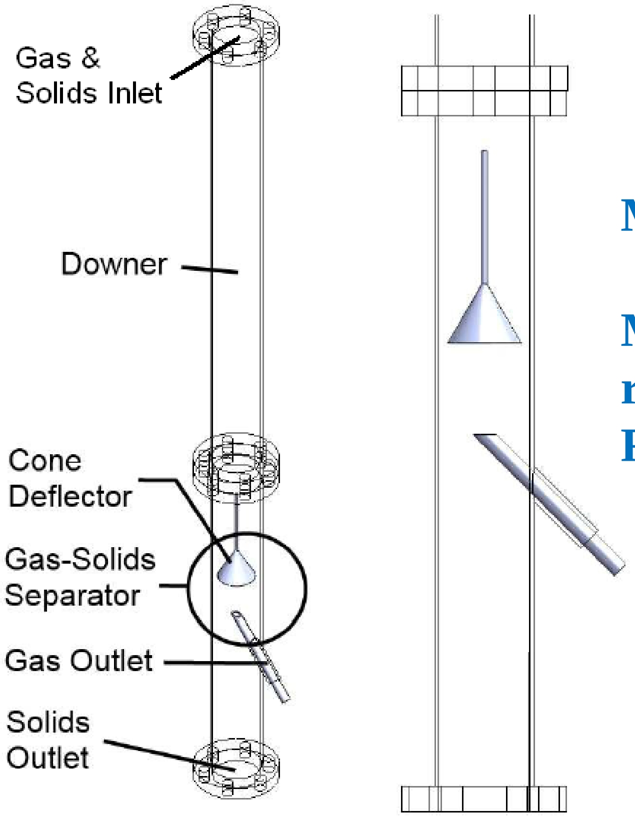

More uniform mixing

More uniform gas phase residence time distribution
Range: <2 seconds

A Novel downer reactor geometry

The institute for Chemical and Fuels from Alternative Resources (ICFAR) at the Western University (Huard et al, 2010)

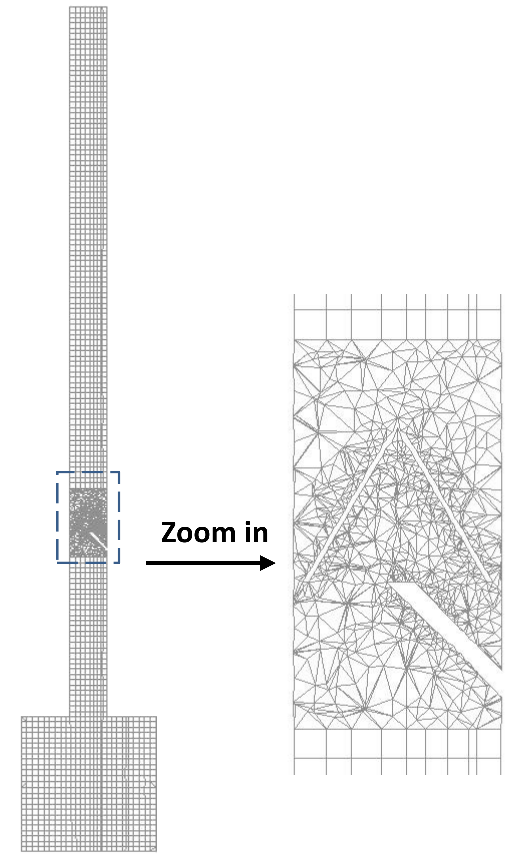

Schematic of calculation domain and mesh

Reference: Martin Huard, Franco Berruti, and Cedric Briens, 2010. Experimental study of a novel fast gas-solid separator for pyrolysis reactors, Vol 8, Article A134 (DOI: 10.2202/1542-6580.1969)

Objectives

Our objectives are to investigate the effect of various separator geometries, operation conditions and particle properties on the separation efficiency in a downer pyrolysis reactor.

To provide optimal operation condition to improve separation efficiency for equipment design and development.

Governing equations: Continuity, Momentum, Energy

Solid phase:

continuity equation: $$\frac{\partial(\alpha_s\rho_s)}{\partial t} + \nabla(\alpha_s\rho_s\vec{u}_s) = 0$$

momentum: $$\frac{\partial(\alpha_s\rho_s\vec{u}_s)}{\partial t} + \nabla(\alpha_s\rho_s\vec{u}_s\vec{u}_s) = -\alpha_s\nabla P - \nabla P_s + \nabla\left(\overline{\overline{\tau}}_s\right) + \beta\left(u_g - u_s\right) + F$$

Gas phase:

continuity equation: $$\frac{\partial\left(\alpha_g\rho_g\right)}{\partial t} + \nabla\left(\alpha_g\rho_g\vec{u}_g\right) = 0$$

momentum: $$\frac{\partial\left(\alpha_g\rho_g\vec{u}_g\right)}{\partial t} + \nabla\left(\alpha_g\rho_g\vec{u}_g\vec{u}_g\right) = -\alpha_g\nabla P + \nabla\left(\overline{\overline{\tau}}_g\right) - \beta\left(u_g - u_s\right) + F$$

Energy equation (granular temperature):

$$\frac{3}{2}\left[\frac{\partial(\alpha_s\rho_s T)}{\partial t} + \nabla(\alpha_s\rho_s T)\vec{u}_s\right] = \left(-P_s\overline{\overline{I}} + \overline{\overline{\tau}}_s\right):\nabla\vec{u}_s - \nabla(\kappa_T\nabla T) - \gamma_T - J_T$$

Gas and solid phase boundary/operating conditions

Boundary/operating condition	Value
Gas mass flowrate, $\dot{m}_g$ [kg/s]	0.0039,0.0239,0.0439
Gas density, ρ_g [kg/m^3]	1.2
Gas dynamic viscosity [kg/(m.s)]	$1.8\text{x}10^{-5}$
Gas outlet pressure, P_{go} [Pa_g]	0
Apparent particle density, ρ_P [kg/m^3]	2650
Solid mass flowrate, $\dot{m}_s$ [kg/s]	0.004, 0.02,0.04,0.08
Particle size, D_s [µm]	60,200
Angle of cone deflector [degree]	60, 90, 120
Separation length, L_s [m]	0, 0.035, 0.07

Model setup for numerical experiment

Granular shear stress	Gidaspow et al.
Diffusion of granular temperature	Gidaspow et al.
Drag	Syamlal and O’Brian
Turbulence	K-epsilon, RSM
Particle-particle restitution	0.9
Particle-wall restitution	0 ~1
Frictional Viscosity	Johnson et al
Bulk viscosity	Lun et al
Solids pressure	Lun et al
Radial distribution function	Ogawa et al
Specularity coefficient	0~1

Eulerian vs Lagrangian

	Eulerian	Lagrangian (Discrete Phase Modeling
Mass loading	Many particles, High mass loading	a fairly low volume fraction, usually less than 10–12%
Governing equations	Continuum equations for both gas and solid phases	Continuum equations for gas phase; the particulate phase is treated as single particles (Newton's second law)
Separation efficiency	Instantaneous monitoring mass flux ratio (output/input) at any time point	At the end of particle tracking duration, mounting number ratio (trapped at the outlet /injection)
Restitution coefficient (particle-wall)	Johnson and Jackson (1987) wall boundary condition: specularity coefficient and the particle–wall restitution coefficient.	Normal and tangential component of the particle–wall restitution coefficient.

Impact of boundary condition at the wall

Discrete phase model in Fluent

Figure 7.3 Particle Track Behavior at a Wall Boundary

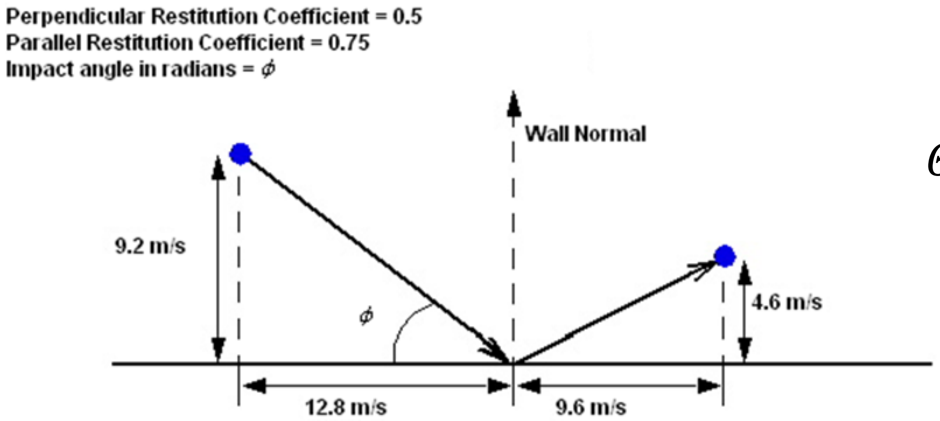

（from ANSYS Fluent 14.0 Manual）

No-slip BC in Fluent

$$v_{S,N} = 0,\ v_{S,T} = 0$$
$$v_{G,N} = 0,\ v_{G,T} = 0$$

Johnson and Jackson (1987)

$$v_{s,w} = -\frac{6\mu_s \alpha_{s,max}}{\sqrt{3\Theta}\pi\varphi\rho_s\alpha_s g_{0,ss}}\frac{\delta v_{s,w}}{\delta n}$$

$$\Theta_s = -\frac{k_s\Theta}{\gamma_w}\frac{\delta\Theta_w}{\delta n} + \frac{\sqrt{3}\pi\varphi\rho_s\alpha_s v_{s,slip}^2 g_{0,ss}\,\Theta^{3/2}}{6\alpha_{s,max}\gamma_w}$$

$$\gamma_w = \frac{\sqrt{3}\pi(1-e_w^2)\rho_s\alpha_s g_{0,ss}\,\Theta^{3/2}}{4\alpha_{s,max}}$$

where φ is the specularity coefficient and e_w is the particle–wall restitution coefficient.

$$v_{S,N} = 0,\ v_{S,T} \neq 0$$
$$v_{G,N} = 0,\ v_{G,T} = 0$$

φ → 0 Zero shear at the wall

φ → 1 A significant amount of Lateral momentum transfer

Separation Mechanism and Force Analysis

$$\frac{\partial(\alpha_s\rho_s\vec{u}_s)}{\partial t}+\nabla(\alpha_s\rho_s\vec{u}_s\vec{u}_s)=-\alpha_s\nabla P-\nabla P_s+\nabla\left(\bar{\bar{\tau}}_s\right)+\beta\left(u_g-u_s\right)+F$$

Gas Pressure
Solid Pressure
Shear stress
Drag force
Gravity

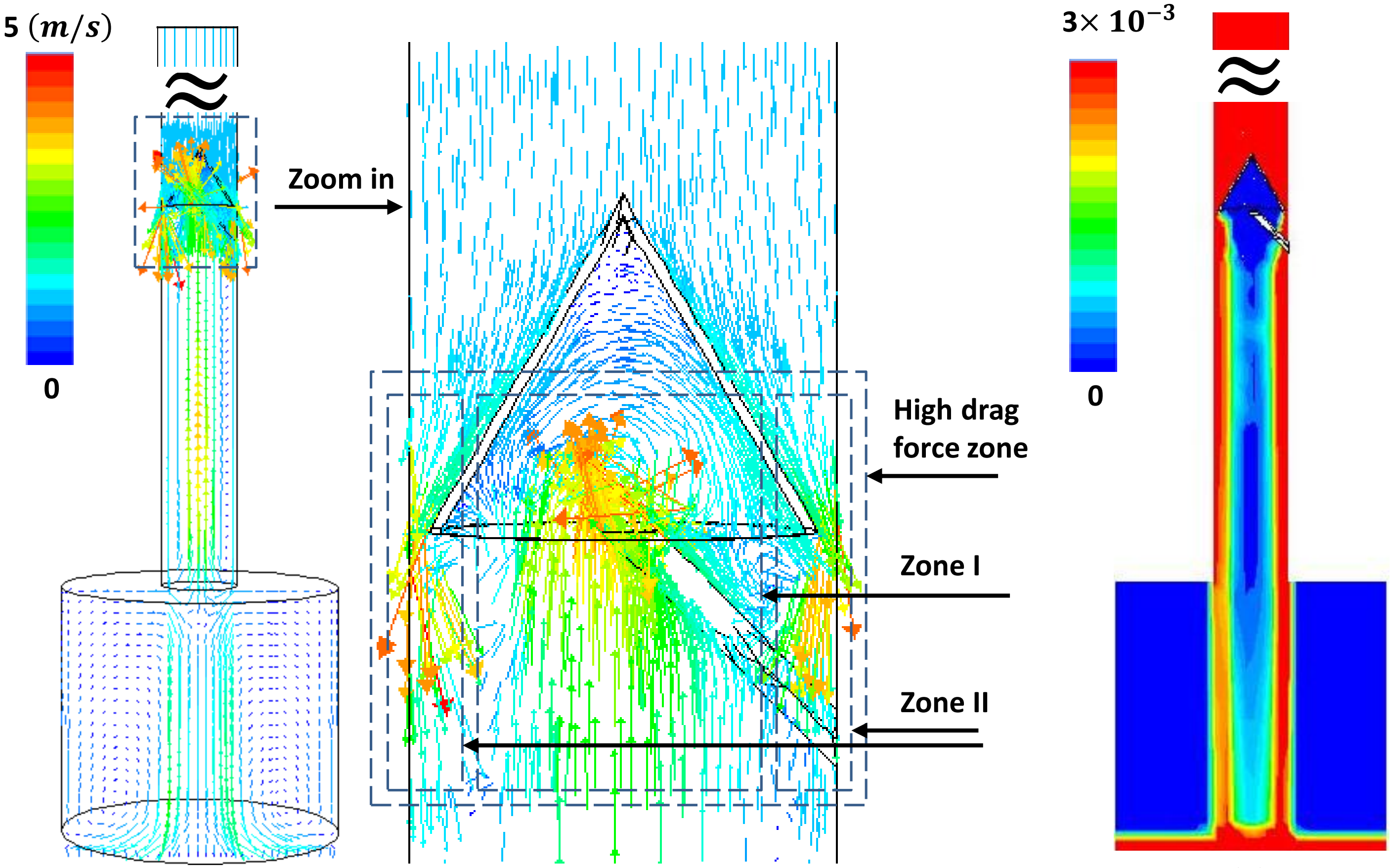

(a) Vector of Gas Velocity

(b) Solid volume fraction

Effect of downstream particle accumulation

solid mass flow rate 0.08kg/s
gas mass flow rate 0.0039kg/s

The boundary condition
$e_{wall} = 0.9, \varphi_{wall} = 0$

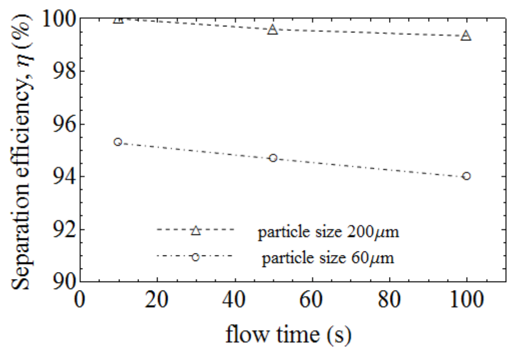

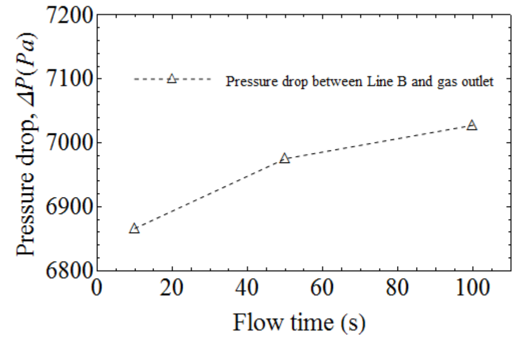

Particle accumulation increasing

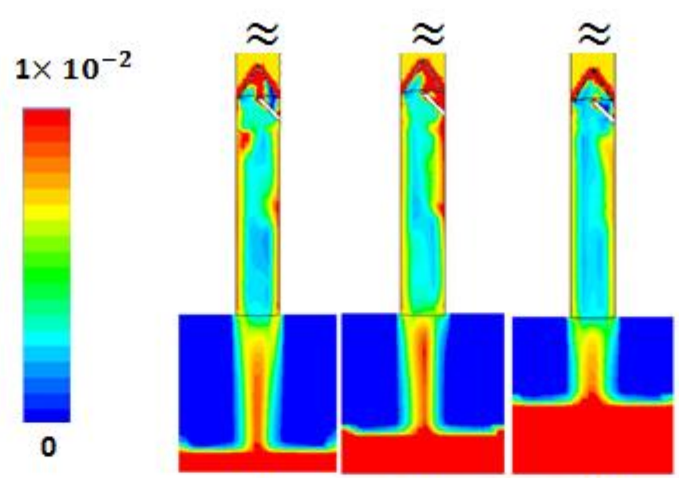

(a) 10s (b) 50s (c) 100s

Solid volume fraction

The result indicated that the effect of downstream particle accumulation was strong, the gas separation efficiency is decreasing due to the effect of pressure change.

Effect of gas inlet velocity

solid mass flow rate 0.004kg/s
gas mass flow rate 0.0039kg/s
Particle size 200μm

The boundary condition
$e_{wall} = 0.9, \varphi_{wall} = 0$

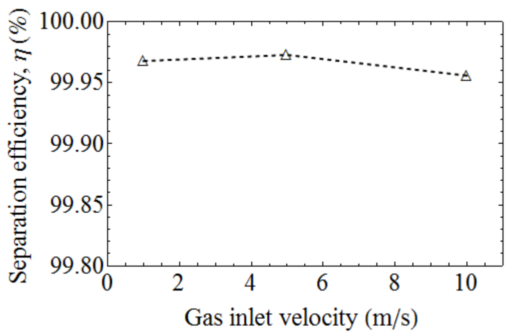

- The effect of gas velocity on separation is weak for large silica sand particle (200 μm).

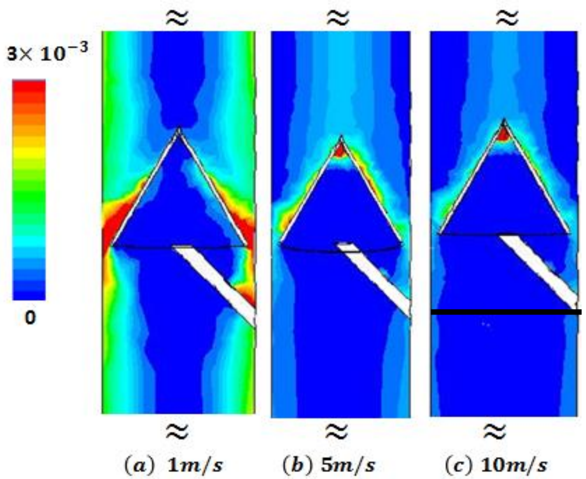

Sample line

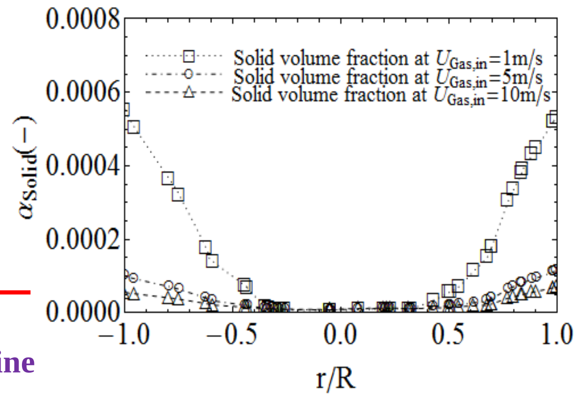

Solid volume fraction

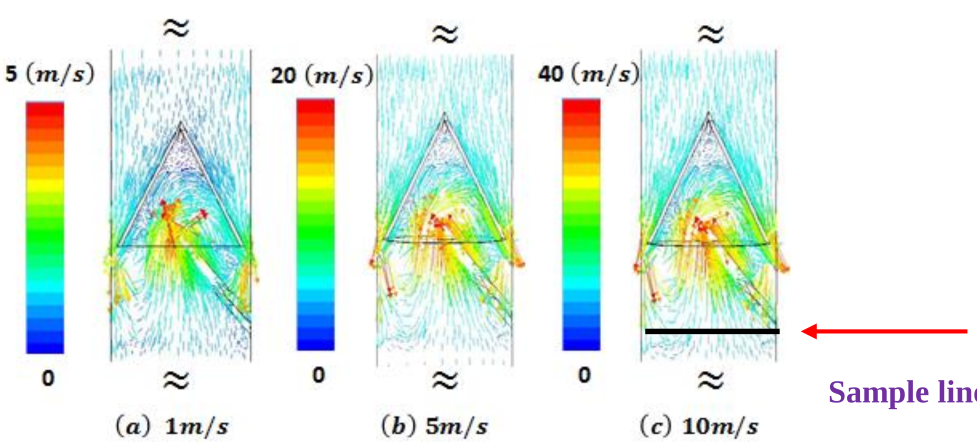

Sample line

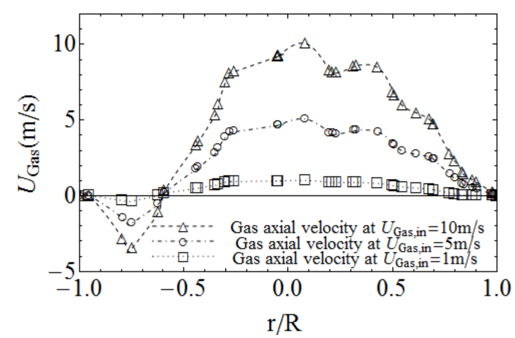

Gas axial velocity

Effect of solid loading

gas mass flow rate 0.0039kg/s
Particle size 60μm

The boundary condition
$e_{wall} = 0.9$, $\varphi_{wall} = 0$

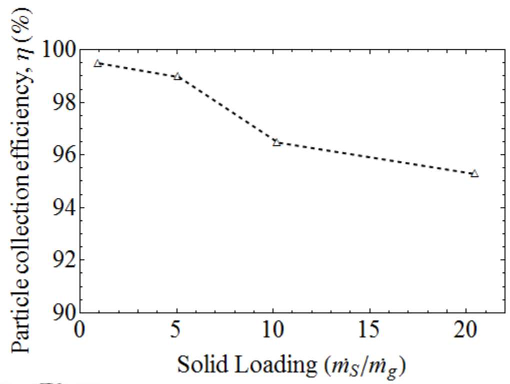

- The separation efficiency is decreasing as solid loading increased.

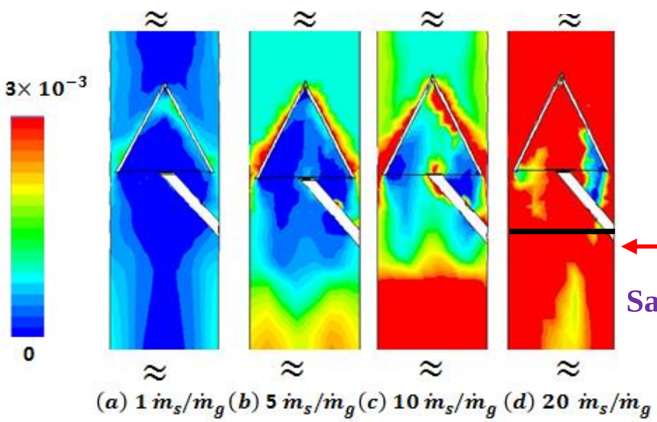

Sample line

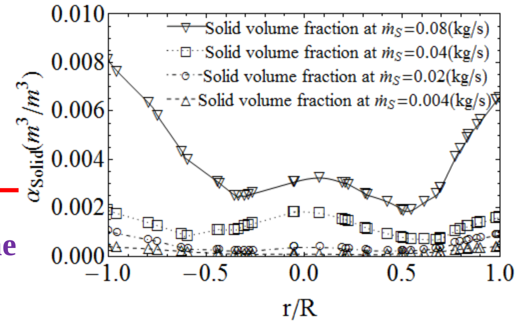

Solid volume fraction

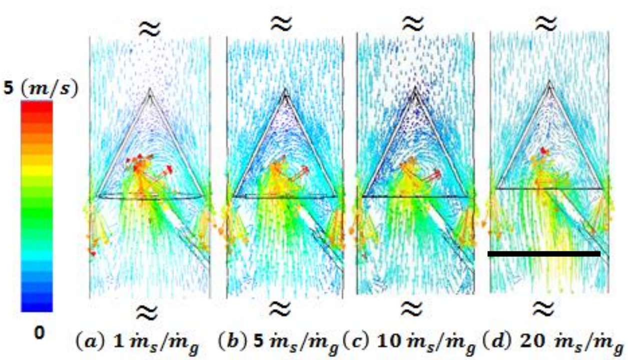

Sample line

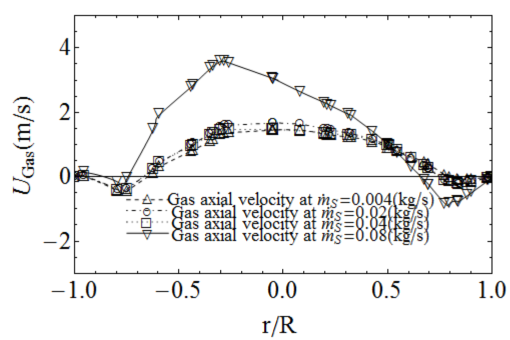

Gas axial velocity

Effect of conical deflector angle

gas mass flow rate 0.0039kg/s
Particle size 60μm

The boundary condition
$e_{wall} = 0.9$, $\varphi_{wall} = 0$

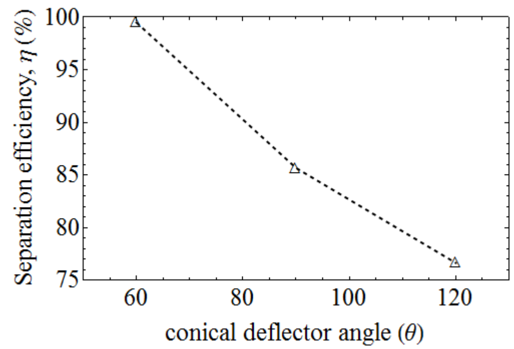

The separation efficiency is decreasing as conical deflector angle increased.

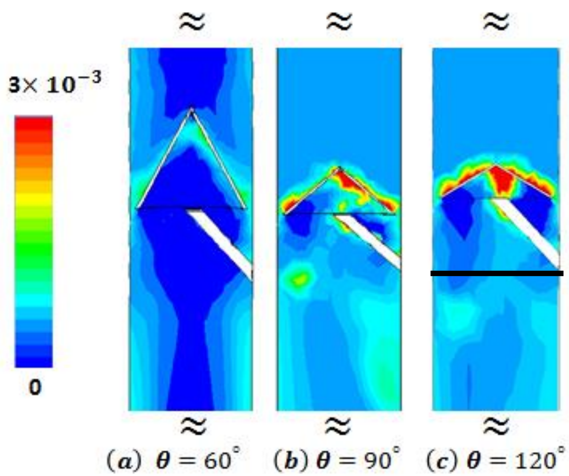

Sample line

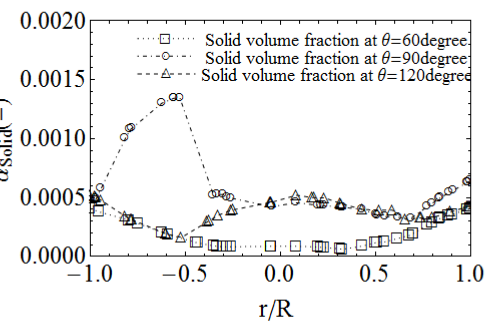

Solid volume fraction

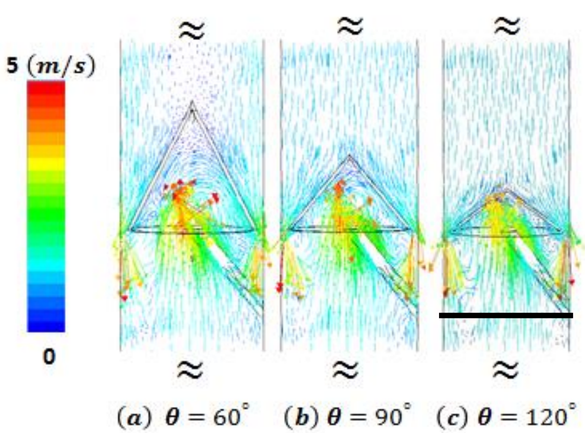

Sample line

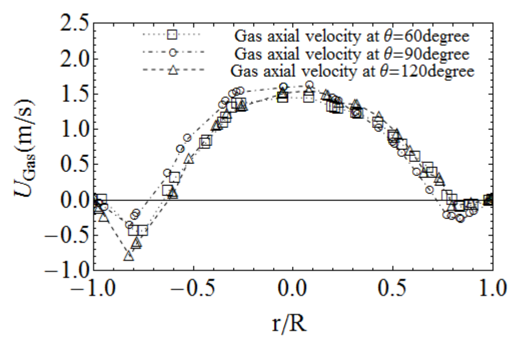

Gas axial velocity

Effect of separation length

gas mass flow rate 0.0039kg/s
Particle size 60μm

The boundary condition
$e_{wall} = 0.9, \varphi_{wall} = 0$

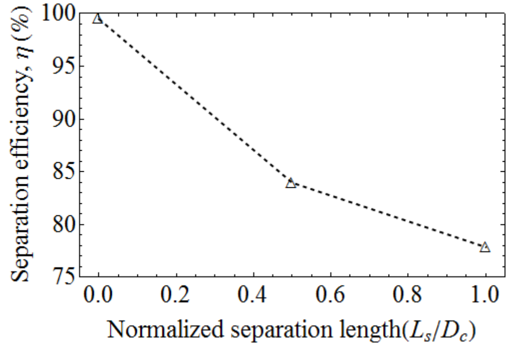

- The separation efficiency is decreasing as separation length increased.

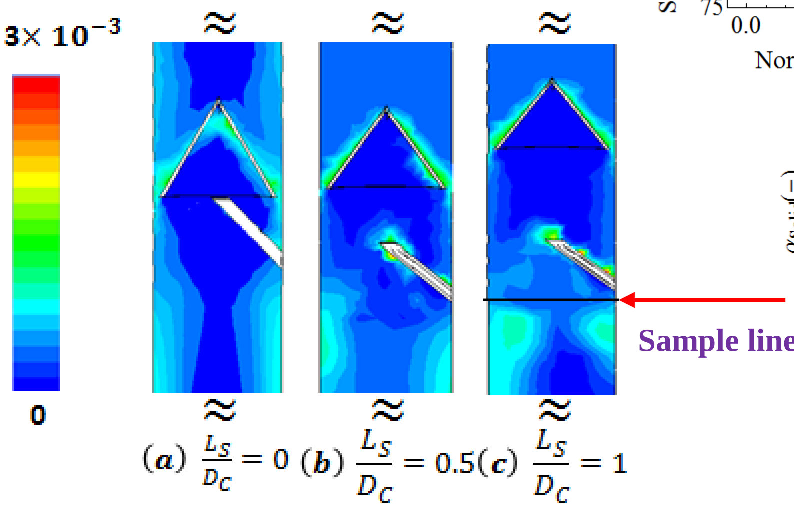

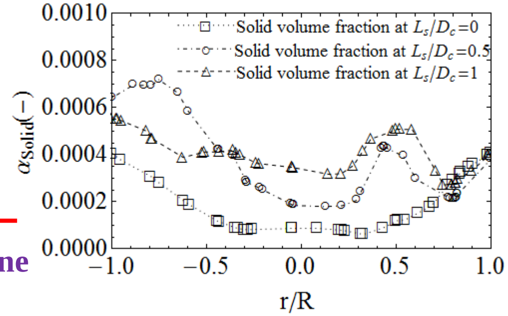

Solid volume fraction

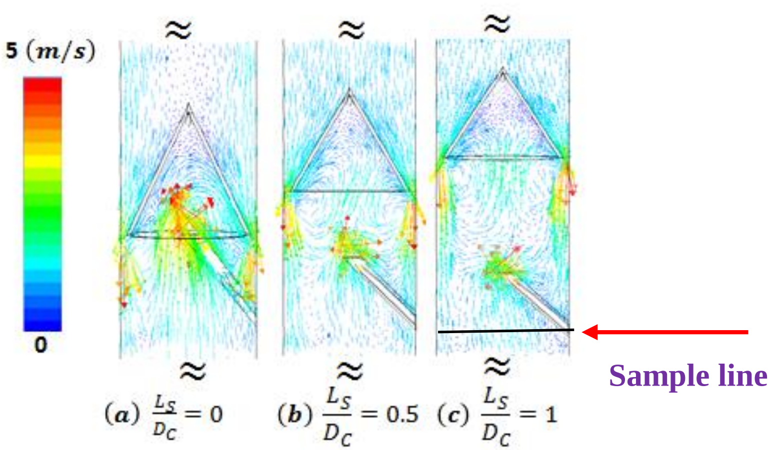

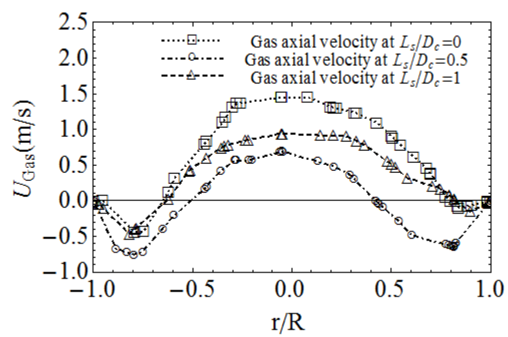

Gas axial velocity

Effect of particle-wall interaction

solid mass flow rate 0.004kg/s
gas mass flow rate 0.0039kg/s

The boundary condition
$e_{wall} = 0.9, \varphi_{wall} = 0$

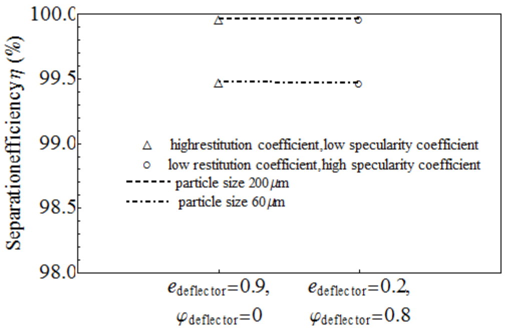

effect of particle-wall interaction at conical deflector on gas separation efficiency

solid mass flow rate 0.004kg/s
gas mass flow rate 0.0039kg/s

The boundary condition
$e_{cone} = 0.9, \varphi_{cone} = 0$

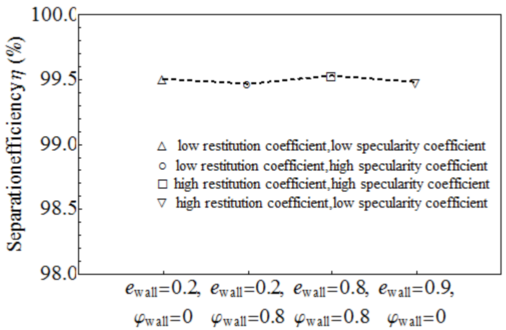

effect of particle-wall interaction on gas separation efficiency

- The effect of particle-wall interaction of conical deflector on separation efficiency is weak

Effect of particle size

Solid loading (kg/s)	Particle size (μm)	Particle collection efficiency (%)
0.08	60	95.270
0.08	200	99.999

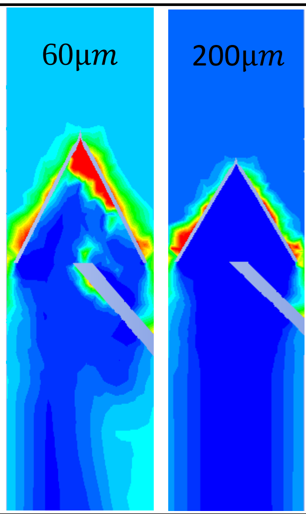

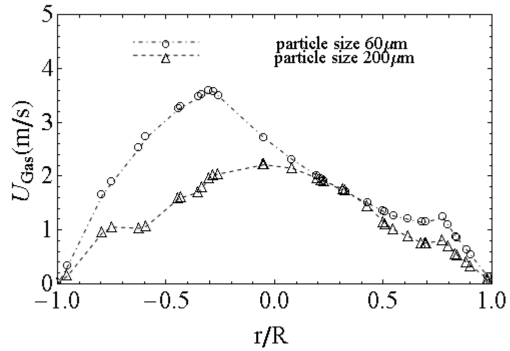

Gas axial velocity

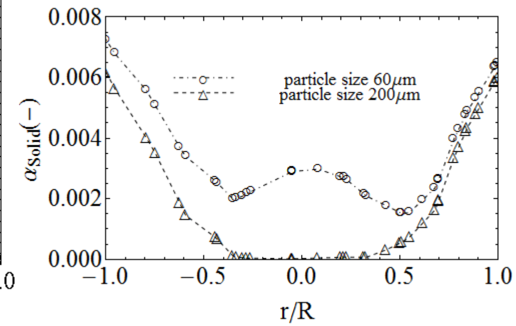

Solid volume fraction

➢ The results indicated that the gas separation efficiency was closely linked to particle size. Small particle (60 μm) can be entrained much more easily by gas flow in gas outlet zone.

Solid loading (kg/s)	Particle size (μm)	Particle collection efficiency (%)
0.004	60	99.483
0.004	200	99.968

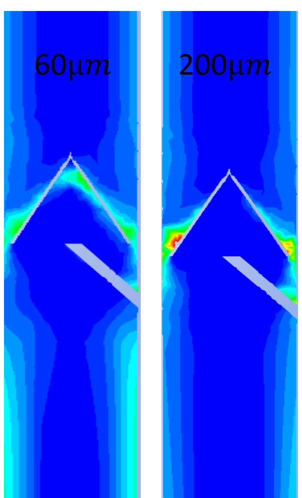

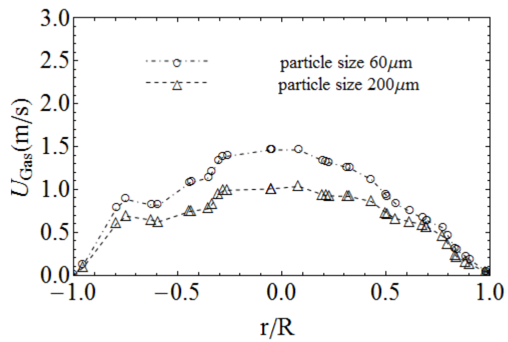

Gas axial velocity

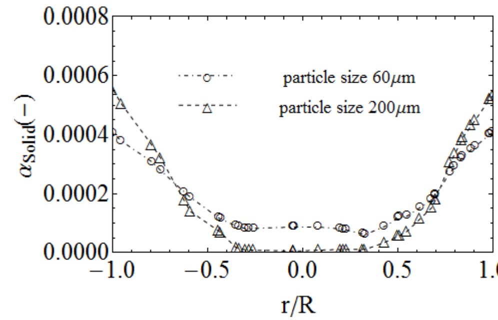

Solid volume fraction

gas mass flow rate 0.0039kg/s

The boundary condition
$e_{wall} = 0.9, \varphi_{wall} = 0$

Summary and Future work

It is concluded that the gas separation efficiency is, to a great extent, independent of the gas inlet velocity and surface properties of the conical separator and wall, but strongly influenced by the solid loading, particle size and geometrical configuration (e.g. separation length, conical deflector angle)

Further work will be on extending the developed hydrodynamic model for the novel downer reactor to simulate hot reactive system for biomass pyrolysis.

Acknowledgement

Aston University
Dr Yassir T. Makkawi

Grant funding from The Leverhulme Trust

Heriot Watt University
Professor Raffaella Ocone

Western University
Professor Franco Berruti
Mr Martin Huard
Professor Cedric Briens